Chimeric RNA ASTN2-PAPPA(as) aggravates tumor progression and metastasis in human esophageal cancer

Wang, Lu; Xiong, Xiao; Yao, Zhimeng; Zhu, Jianlin; Lin, Yusheng; Lin, Wan; Li, Kai; Xu, Xiaozheng; Guo, Yi; Chen, Yuping

Published in:
Cancer letters

DOI:
10.1016/j.canlet.2020.10.052

Publication date:
2021

Cancer Letters 501 (2021) 1–11

Contents lists available at ScienceDirect

Cancer Letters

journal homepage: www.elsevier.com/locate/canlet

Chimeric RNA ASTN2-PAPPA$_{as}$ aggravates tumor progression and metastasis in human esophageal cancer

Lu Wang [a], Xiao Xiong [a], Zhimeng Yao [a], Jianlin Zhu [a], Yusheng Lin [a,b], Wan Lin [c], Kai Li [a], Xiaozheng Xu [d], Yi Guo [e], Yuping Chen [f], Yunlong Pan [a], Fuyou Zhou [g,h], Jun Fan [i], Yan Chen [i], Shegan Gao [j,**], Sai-Ching Jim Yeung [k,l], Hao Zhang [a,*]

[a] Department of General Surgery, The First Affiliated Hospital of Jinan University, Institute of Precision Cancer Medicine and Pathology, School of Medicine, Jinan University, Guangzhou, Guangdong, China
[b] Department of Hematology, University Medical Center Groningen, University of Groningen, Groningen, the Netherlands
[c] Cancer Research Center, Shantou University Medical College, Shantou, Guangdong, 515041, China
[d] Division of Biological Sciences, University of California San Diego, La Jolla, CA, USA
[e] Endoscopy Center, Affiliated Cancer Hospital of Shantou University Medical College, Shantou, Guangdong, China
[f] Department of Thoracic Surgery, Affiliated Cancer Hospital of Shantou University Medical College, Shantou, Guangdong, China
[g] The Fourth Affiliated Hospital of Henan University of Science and Technology, Anyang, Henan, 455001, China
[h] Department of Thoracic Surgery, Anyang Tumor Hospital, Anyang, Henan, 455001, China
[i] Department of Medical Biochemistry and Molecular Biology, School of Medicine, Jinan University, Guangzhou, 510632, China
[j] College of Clinical Medicine, The First Affiliated Hospital of Henan University of Science and Technology, Henan Key Laboratory of Cancer Epigenetics, Luoyang, 471003, China
[k] Department of Emergency Medicine, University of Texas MD Anderson Cancer Center, Houston, TX, USA
[l] Department of Endocrine Neoplasia and Hormonal Disorders, University of Texas MD Anderson Cancer Center, Houston, TX, USA

ARTICLE INFO

Keywords:
Chimeric RNA
Esophageal squamous cell carcinoma
Stemness
Metastasis

ABSTRACT

Transcription-induced chimeric RNAs are an emerging area of research into molecular signatures for disease biomarker and therapeutic target development. Despite their importance, little is known for chimeric RNAs-relevant roles and the underlying mechanisms for cancer pathogenesis and progression. Here we describe a unique ASTN2-PAPPA$_{antisense}$ chimeric RNA (A-P$_{as}$chiRNA) that could be the first reported chimeric RNA derived from the splicing of exons and intron antisense of two neighboring genes, respectively. Aberrant A-P$_{as}$chiRNA level in ESCC tissues was associated with tumor progression and patients' outcome. In vitro and in vivo studies demonstrated that A-P$_{as}$chiRNA aggravated ESCC metastasis and enhanced stemness through modulating OCT4. Mechanistic studies demonstrated that ERK5-mediated non-canonical PAF1 activity was required for A-P$_{as}$chiRNA-induced cancer malignancy. The study defined an undocumented function of chimeric RNAs in aggravating cancer stemness and metastasis.

1. Introduction

Chimeric RNAs are traditionally thought to be products of gene fusions, and thus, are thought to be unique features of neoplasia [1,2]. With recent advances in next-generation RNA sequencing and bioinformatics, mechanisms driving the production of chimeric RNAs besides gene fusion have been discovered, such as transcriptional read-through and alternative RNA splicing [1,3,4]. It is hypothesized that chimeric RNAs may exert a novel layer of cellular complexity that contributes to cancer evolution and malignancy, and have potentials as molecular biomarkers and therapeutic targets [5,6]. Even though plenty of chimeric RNAs have been discovered and reported in cancers, their functions in the cancer pathogenesis and progression have largely unknown.

Our previous studies indicated that chimeric RNAs were undetectable in normal esophagus while was highly expressed in human esophageal squamous cell carcinoma (ESCC), which is the third most

* Corresponding author. Institute of Precision Cancer Medicine and Pathology, School of Medicine, Jinan University, 601 Huangpu Avenue West, Guangzhou, Guangdong, 510632, China.
** Corresponding author.
E-mail addresses: gsg112258@163.com (S. Gao), haolabcancercenter@163.com (H. Zhang).

https://doi.org/10.1016/j.canlet.2020.10.052
Received 31 July 2020; Received in revised form 26 October 2020; Accepted 29 October 2020
Available online 31 December 2020

common cancer of the gastrointestinal tracts and the sixth leading cause of cancer-related deaths globally [7,8]. One of the chimeric RNAs, was

Abbreviations

ASTN2	Astrotactin-2
PAPPA	Pappalysin 1
PAPPAas	Antisense DNA Complementary to The DNA Sequence Coding for Pappalysin 1
IGFBP	Insulin-Like Growth Factor-Dependent IGF Binding Protein-4 Protease
ESCC	Esophageal Squamous Cell Carcinoma
CSCs	Cancer Stem Cells
ESCs	Embryonic Stem Cells
OCT4	Octamer-Binding Protein 4
ERK5	Extracellular-Signal-Regulated Kinase 5
EGFR	Epidermal Growth Factor Receptor
PAF1	RNA Polymerase II-Associated Factor 1 Homolog
SOX2	SRY-Box Transcription Factor 2
KLF4	Kruppel Like Factor 4
KLF5	Kruppel Like Factor 5
GEO	Gene Expression Omnibus
GSEA	Gene Set Enrichment Analyses
FDR	False Discovery Rate
CNVs	Copy Number Variants
RTCA	Real-Time Cell Analyzer System

related to the ASTN2 and PAPPA genes, and hence, was initially named ASTN2-PAPPA [7]. This chimeric RNA has been suggested to be generated by transcription read-through/splicing or trans-splicing, but not by mutational events that produce a fusion gene [9]. ASTN2, coding for the Astrotactin 2 protein, is highly expressed in the brain and functions in neuronal migration [10]. Recently, the copy number variants (CNVs) of ASTN2, both deletions and duplications, were identified in patients with neurodevelopmental disorders, including autism spectrum disorder, schizophrenia, attention-deficit/hyperactivity disorder, bipolar disease, intellectual disability, and global developmental delay [11,12]. PAPPA encodes a secreted metalloproteinase, Pappalysin 1, which cleaves insulin-like growth factor binding proteins (IGFBPs) [13]. PAPPA plays a role in bone formation, inflammation, wound healing and female fertility [14]. Enhanced expression of PAPPA is associated with diabetic nephropathy, and may promote invasion and growth of various human cancers [15,16].

The biological function of chimeric RNA involving ASTN2 has not been studied before. In this study, we analyzed the nucleotide sequence of the cDNA of the chimeric RNA involving ASTN2 and PAPPA to shed light on potential mechanisms of its generation and investigated the potential roles and relevant mechanism of this chimeric RNA in human ESCC, where cancer stemness is critical for its development, metastasis and recurrence [5,17–21].

2. Materials and methods

2.1. Patient tissue samples

A total of 78 specimens were histopathologically and clinically diagnosed as ESCC and obtained from the Affiliated Tumor Hospital of Shantou University Medical College from 2010 to 2012. Patients who had undergone preoperative radiotherapy or chemotherapy were excluded from this study. Clinical research protocols of this study were reviewed and approved by the Ethics Committee of Shantou University Medical College.

2.2. Long-range PCR

LA PCR kit (Takara) was used for long-range PCR analysis of patient genomic DNA as previously described [7]. To ensure that the PCR primers designed can amplify the intended DNA fragment, we used commercial human genomic DNA (Promega) as a control. Primers used are listed below.

No.	Forward	Reverse
1	CTGGGTTATCCATGTGCCCC	GCATGGTGCAAGGGGAAAAG
2	CTTTTCCCCTTGCACCATGC	GGGAAGGTTCATGGGGACTG
3	GATGGGGTTCCTCAGGGGA	GGGGGTAGGGCTGAAGTCTA
4	CTTTTCCCCTTGCACCATGC	AGCAGAGAAGAAAGGCACCC
5	ATTTGGGGCCGCTTTTTCAC	GGGAAGGTTCATGGGGACTG
6	TAGACTTCAGCCCTACCCCC	TACTTCCCTCAGGGTCGGAG

2.3. In situ hybridization

Nonradioactive in situ hybridization was performed as described previously [7]. In brief, antisense RNA probes labeled with digoxigenin were transcribed from cDNA templates. Paraffin-fixed tissue sections from ESCC were deparaffinized, treated with proteinase K, pre-hybridized and then hybridized with probes. Following hybridization, the slides were washed and treated with a blocking reagent and then incubated with anti-digoxigenin and detected as detailed. Antisense probes were designed against the fusion junction or RNA segments specific to these chimeric RNAs, so as to distinguish chimeric RNAs from the parental mRNAs. We tested and confirmed the specificity of the antisense probes to distinguish chimeric RNAs from parental mRNA using dot blot assay. Antisense probe specific to chimeric RNA of interest but to neither the parental gene ASTN2 nor PAPPA: (gtaatacgactcactatagg) CATCCTTTTTTGAAGATGAAAACACATGCCCTCAGATAGCAGAAGTTCTTCACTGTAACTTA-CAGTGGGAATCAGCACTCTTGTGTTTAGCCCAGGA-CACTGGCT*CGTGTTTCG.

2.4. Cell proliferation assay

Cell proliferation assay was performed in a real-time cell analyzer system (RTCA, Roche Applied Science, Mannheim, Germany) [18]. Cells were trypsinized and resuspended in culture medium. Background measurements were taken from the wells by adding 50 μL of the same medium to the E−16 plates. Subsequently, cells were plated at a density of 2000/well in fresh medium to a final volume of 150 μL. Cells were incubated for 30 min at the clean bench before the software schedule was initiated. The impedance signals were recorded every 15 min until the end of the experiment.

2.5. Migration and invasion

Cell migration and invasion assays were conducted using the xCELLigence RTCA Analyzer. Briefly, 150 μL of RPMI-1640 supplemented with 10% FBS was added to the lower chamber in the CIM-16 plate (16-well, 8-μm pore filter) and 3×10^4 cells in 100 μL of serum-free RPMI-1640 were added to the upper chamber coated with or without Matrigel (BD Biosciences, USA). The impedance signals were recorded every 15 min until the end of the experiment.

2.6. Immunofluorescence

Immunofluorescence was performed as described previously [18,22]. Briefly, cells were grown on glass cover slips, fixed in 4% PFA for 20 min. The cells were stained with rabbit anti-CD44 antibody (Cat. No. 3570, Cell Signaling Technology) overnight at 4 °C. Secondary antibodies were incubated with Alexa-Fluor-488 (Green)-conjugated donkey anti-mouse antibodies (Cat. No. A-11055, Invitrogen). Cells

were mounted in ProLong™ Gold Antifade Mountant with DAPI (Cat. No. P36935, Invitrogen). Samples were examined under a confocal fluorescence microscope (FV-1000; Olympus, Japan).

3. Results

3.1. Structure of chimeric RNA involving ASTN2 and PAPPA and possible mechanisms of its formation

We previously demonstrated that one of ESCC-enriched chimeric RNAs involved the ASTN2 and PAPPA genes [7]. ASTN2, PAPPA, PAPPA-AS1 and PAPPA-AS2 are genes in close proximity on chromosome 9 (Fig. 1B). PAPPA is on the plus strand of chromosome 9, while ASTN2, PAPPA-AS1 and PAPPA-AS2 are on the minus strand. The nucleotide sequence of the cDNA of the chimeric RNA consists of the full-length coding sequence of the ASTN2 gene, the subsequent nucleotide sequence corresponds to the antisense strand of part of 18th intron of the PAPPA gene (i.e., 5′-AGCCAGTGTCCTGGGCTAAACACAA-GAGTGCTGATTCCCACTGTAAGTTACAGTGAA-GAACTTCTGCTATCTGAGGGCATGTGTTTTCATCTTCAAAAAAGGATG-GACAGTCCCCATGAACCTTCCCTCTCCAACCACA-CAGGCCTTGCTTCTGGACATGCAGTGA-TAACTCTCTGTTTGCTGGATGAAGATCATGTTGGCTCTATGCACATTC-AGATAACCTTCTACACCAGACACCCCTGG-3′ as determined experimentally by RT-PCR sequencing). This chimeric mRNA is predicted to be translated into a protein that has the N-terminal portion of the full-length ASTN2 protein, and the subsequent 81 new amino acids at the C-terminal portion are in a novel sequence that does not correspond to any part of the PAPPA protein. Therefore, we refer to this chimeric RNA as ASTN2-PAPPA$_{antisense}$ chimeric RNA (A-P$_{as}$chiRNA) hereafter.

Since PAPPA is on the plus strand of DNA and ASTN2 is on the minus strand of chromosome 9 DNA in a head-to-head configuration, several possibilities for the mechanism of formation of A-P$_{as}$chiRNA remain:

a) Transcription read-through of ASTN2 with splicing of the RNA transcript to result in A-P$_{as}$chiRNA.
b) Transcription read-through of PAPPA-AS1 such that the transcript contains the antisense portion of 18th intron of PAPPA. Then, cis-SAGe or trans-splicing of ASTN2 transcript and the elongated PAPPA-AS1 can result in A-P$_{as}$chiRNA.

To clarify whether A-P$_{as}$chiRNA is generated from a fusion chimeric

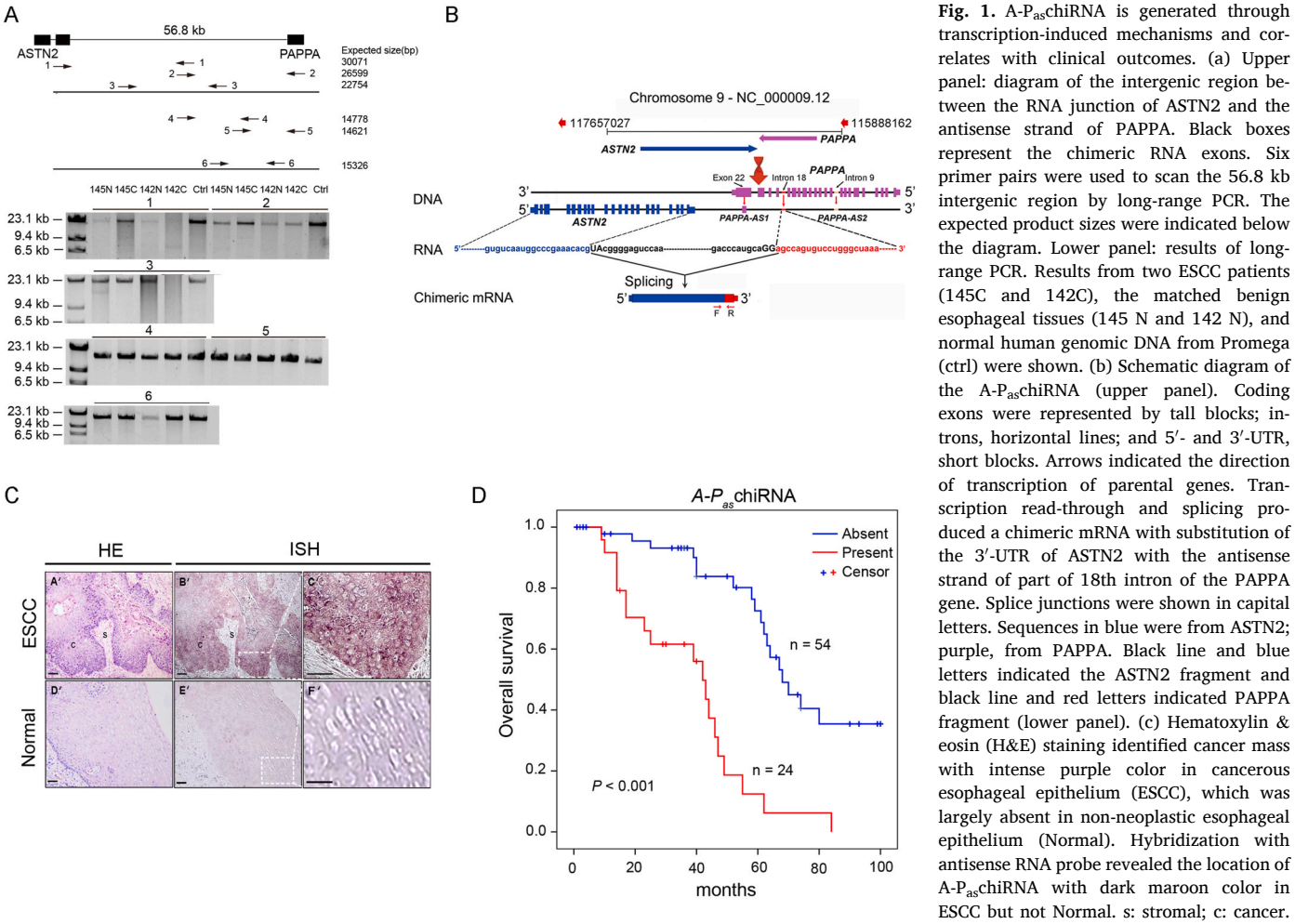

Fig. 1. A-P$_{as}$chiRNA is generated through transcription-induced mechanisms and correlates with clinical outcomes. (a) Upper panel: diagram of the intergenic region between the RNA junction of ASTN2 and the antisense strand of PAPPA. Black boxes represent the chimeric RNA exons. Six primer pairs were used to scan the 56.8 kb intergenic region by long-range PCR. The expected product sizes were indicated below the diagram. Lower panel: results of long-range PCR. Results from two ESCC patients (145C and 142C), the matched benign esophageal tissues (145 N and 142 N), and normal human genomic DNA from Promega (ctrl) were shown. (b) Schematic diagram of the A-P$_{as}$chiRNA (upper panel). Coding exons were represented by tall blocks; introns, horizontal lines; and 5′- and 3′-UTR, short blocks. Arrows indicated the direction of transcription of parental genes. Transcription read-through and splicing produced a chimeric mRNA with substitution of the 3′-UTR of ASTN2 with the antisense strand of part of 18th intron of the PAPPA gene. Splice junctions were shown in capital letters. Sequences in blue were from ASTN2; purple, from PAPPA. Black line and blue letters indicated the ASTN2 fragment and black line and red letters indicated PAPPA fragment (lower panel). (c) Hematoxylin & eosin (H&E) staining identified cancer mass with intense purple color in cancerous esophageal epithelium (ESCC), which was largely absent in non-neoplastic esophageal epithelium (Normal). Hybridization with antisense RNA probe revealed the location of A-P$_{as}$chiRNA with dark maroon color in ESCC but not Normal. s: stromal; c: cancer. Scale bar = 100 μm. (d) Kaplan-Meier analysis showed that the OS was significantly better in patients without A-P$_{as}$chiRNA than those with A-P$_{as}$chiRNA ($P < 0.001$, log rank test). (For interpretation of the references to color in this figure legend, the reader is referred to the Web version of this article.)

gene or simply produced through RNA processing events, we performed long-range PCR on the genomic DNA isolated from patients' tissues that expressed the corresponding chimeric RNA. The assay yielded indistinguishable product sizes between ESCC tissue, matched benign tissue, and normal human genomic DNA control, indicating that there were no apparent DNA rearrangements in ESCC tissues to a large degree that is detectable by long-range PCR (Fig. 1A). Intriguingly, the genomic nucleotide sequence immediately downstream of the ASTN2 sequence in the chimeric RNA and the genomic nucleotide sequence immediately upstream of the antisense portion of 18th intron of the PAPPA contains a discernable 5′ splice site and a 3' splice site at the RNA junction, respectively (Fig. 1B). This evidence strongly suggests that A-P$_{as}$chiRNA results from RNA splicing.

Because the transcription of a chimeric RNA generated by read-through/splicing is controlled by the promoter of the 5′ parental gene, the higher level of chimera in cancer raised the question if this is because that the 5′ parental genes (ASTN2) is over-expressed in ESCC? To answer this question, we analyzed the available ESCC microarray gene expression database. By retrieving data from Oncomine, we found that the 5′ parental gene ASTN2 was over-expressed in cancer tissue vs. matched benign tissue (fold change = 3.4) while the expression of 3' parental gene PAPPA remained unchanged (Supplementary Fig. 1A). Moreover, there was a positive correlation between the number of copies of A-P$_{as}$chiRNA and the level of mRNA gene expression of ASTN2 (Pearson correlation: r = 0.6374, P = 0.0002), but not any significant correlation between A-P$_{as}$chiRNA and PAPPA (r = 0.1713, P = 0.3655) (Supplementary Fig. 1B). This positive correlation suggested that the generation of A-P$_{as}$chiRNA might be related to the promoter activity for ASTN2 transcription.

Collectively, the observed splice site at RNA junctions, and the lack of evidence of large-scale DNA-level rearrangements, together with the fact that these paired genes are adjacent genes in the genome, suggests that the chimera is likely generated by transcription read-through followed by splicing at the RNA level.

3.2. A-P$_{as}$chiRNA level correlates with tumor progression and predicts clinical outcomes of ESCC patients

To determine the cellular origin localization of A-P$_{as}$chiRNA within ESCC, we performed in situ hybridization using antisense probes against the chimeric junctions and segments specific to A-P$_{as}$chiRNA, revealing that the expression of A-P$_{as}$chiRNA is largely restricted to cancer cells in patient tumors and undetectable in non-neoplastic esophageal tissue (Fig. 1C). To explore the clinical importance of A-P$_{as}$chiRNA in cancer, we performed RT-qPCR assay to validate the prevalence of A-P$_{as}$chiRNA in 78 ESCC patients and correlated its expression with clinicopathological parameters. Aberrant A-P$_{as}$chiRNA was associated with histologic differentiation and lymph node metastasis (P < 0.001 and P = 0.014, respectively; Table 1) but without significant statistical correlation with any other clinicopathological indicators. Importantly, Kaplan-Meier analysis showed patients with A-P$_{as}$chiRNA-expressed ESCC were associated with poorer prognosis (P < 0.001, log rank test; Fig. 1D) and multivariate Cox regression analysis revealed that A-P$_{as}$chiRNA was an independent prognostic factor for overall survival of patients (hazard ratio [HR] 4.08; 95% confidence interval [CI] 1.81 to 9.18; P = 0.001; Table 2). Together, these data demonstrated that A-P$_{as}$chiRNA was of prognostic importance, suggesting that A-P$_{as}$chiRNA might possess a promoting role in ESCC malignancy.

3.3. A-P$_{as}$chiRNA promotes ESCC cell metastasis and stemness through modulating OCT4

In accordance with A-P$_{as}$chiRNA expression in ESCC patients, RT-qPCR assay demonstrated that in 6 out of 14 ESCC cell lines the transcription of A-P$_{as}$chiRNA was restricted to ESCC cell lines and undetectable in 4 immortalized normal esophageal epithelial cell lines

Table 1
Relationship between A-P$_{as}$chiRNA mRNA expression and clinicopathologic variables in human ESCC.

Variables	n	A-P$_{as}$chiRNA		P
		Present, No. (%)	Absent, No. (%)	
Patients	78	24 (30.8)	54 (69.2)	
Gender				
Male	62	22 (35.5)	40 (64.5)	0.076
Female	16	2 (12.5)	14 (87.5)	
Age (years)	78	57.58 ± 7.46	59.85 ± 8.36	0.132
Esophageal location				
Upper/Middle	69	21 (25.0)	48 (75.0)	0.859
Lower	9	3 (31.8)	6 (68.2)	
Largest tumor dimension (cm)	78	6.05 ± 1.54	5.59 ± 1.25	0.215
Histological differentiation				
Well	19	5 (26.3)	14 (73.7)	<0.001
Moderately	44	7 (15.9)	37 (84.1)	
Poorly	15	12 (80.0)	3 (20.0)	
Tumor depth				
T1/T2	14	4 (28.6)	10 (71.4)	0.844
T3/T4	64	20 (31.2)	44 (68.8)	
Lymph node metastasis				
Negative	39	7 (17.9)	32 (82.1)	0.014
Positive	39	17 (43.6)	22 (56.4)	
Stage				
I/II	26	6 (23.1)	20 (76.9)	0.298
III	52	18 (34.6)	34 (65.4)	

P value by chi-square test.

Table 2
Univariate and multivariate Cox proportional hazards model predicting survival in ESCC.

Variables	Univariate analysis		Multivariate analysis	
	HR (95% CI)	P	HR (95% CI)	P
Age (years)				
>60 vs. ≤60	0.92 (0.48–1.75)	0.792	1.10 (0.53–2.30)	0.802
Gender				
Male vs. Female	0.95 (0.39–2.31)	0.913	0.85 (0.32–2.23)	0.733
Histological differentiation				
Poor vs. Well/ Moderate	0.87 (0.44–1.69)	0.280	0.74 (0.28–1.96)	0.547
Largest tumour dimension				
>5 cm vs. ≤ 5 cm	1.15 (0.59–2.24)	0.690	0.72 (0.33–1.56)	0.402
Location of tumors				
Upper/Middle vs. Lower	0.90 (0.35–2.34)	0.835	1.28 (0.38–4.31)	0.685
Tumor depth				
T3/T4 vs. T1/T2	0.88 (0.37–2.12)	0.780	0.39 (0.12–1.25)	0.114
Lymph node metastasis				
Positive vs. Negative	2.14 (1.05–4.35)	0.036	2.25 (0.73–6.99)	0.161
Tissue A-P$_{as}$chiRNA level				
Present vs. Absent	4.91 (2.47–9.73)	<0.001	4.08 (1.81–9.18)	0.001

HR, hazard ratio; CI, confidence interval.

(Fig. 2A). To gain insights into the potential role of A-P$_{as}$chiRNA in ESCC progression, we constructed stable A-P$_{as}$chiRNA overexpression (A-P$_{as}$) and A-P$_{as}$chiRNA knockdown (shA-P$_{as}$) cells using HKESC-2 and HKESC-3 respectively. Cell proliferation monitored by RTCA showed that either depletion or overexpression of A-P$_{as}$chiRNA did not obviously affect cell proliferation in both cells, compared with the control cells (Fig. 2B). Notably, A-P$_{as}$chiRNA depletion drastically suppressed cell migration and invasion (P < 0.05 and P < 0.001, respectively; Fig. 2C), while A-

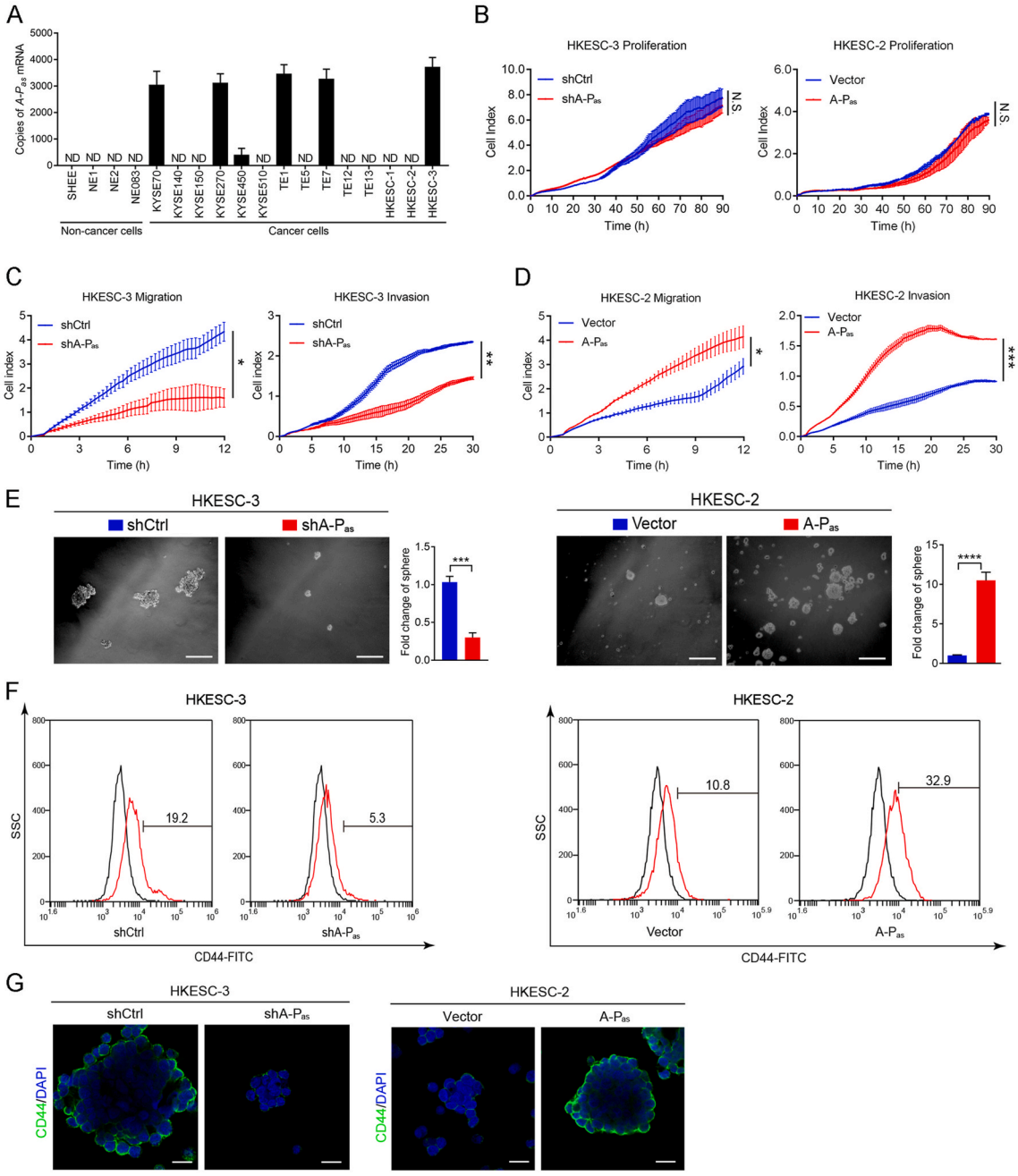

Fig. 2. A-P$_{as}$chiRNA promotes ESCC cell metastatic potency and cancer stemness. (a) The mRNA levels of A-P$_{as}$chiRNA in a panel of ESCC cell lines and four immortalized esophageal epithelial cell lines were measured by RT-qPCR. (b) Proliferation of A-P$_{as}$chiRNA-knockdown HKESC-3 (HKESC-3-shA-P$_{as}$) cells (left panel) and A-P$_{as}$chiRNA-overexpression HKESC-2 (HKESC-2-A-P$_{as}$) cells (right panel) were monitored by the xCELLigence RTCA dual-plate (DP) system for 90 h. (c) Migration (left panel) and invasion (right panel) of HKESC-3-shA-P$_{as}$ cells were monitored by the xCELLigence RTCA DP system for 12 h and 30 h, respectively. (d) Migration (left panel) and invasion (right panel) of HKESC-2-A-P$_{as}$ cells were monitored by the xCELLigence RTCA DP system for 12 h and 30 h, respectively. (e) Representative images of spheres formed by HKESC-3-shA-P$_{as}$ cells (left panel) or HKESC-2-A-P$_{as}$ cells (right panel). Scale bars: 100 μm. Histograms showing the fold change in the number of spheres formed by the indicated cells. (f) Flow cytometry analysis of the CD44^{+} population in HKESC-3-shA-P$_{as}$ cells (left panel) and HKESC-2-A-P$_{as}$ cells (right panel). (g) Immunofluorescent staining of CD44 in the above-mentioned cells. CD44 was labeled in green and nuclei were stained with DAPI (blue). Scale bars: 40 μm. Data are shown as the means of three independent experiments or representative data. Error bars indicate SD. N.S., not statistically significant. *P < 0.05, **P < 0.01, ***P < 0.001 by Student's t-test. (For interpretation of the references to color in this figure legend, the reader is referred to the Web version of this article.)

P$_{as}$chiRNA overexpression acted inversely, as monitored by RTCA (P < 0.05 and P < 0.001 respectively; Fig. 2D). These data collectively demonstrated that A-P$_{as}$chiRNA possessed a promoting role for ESCC metastatic potency. Since our clinical analysis revealed the association of A-P$_{as}$chiRNA with ESCC differentiation, we speculated that the role of A-P$_{as}$chiRNA is involved by cancer stemness that is associated with differentiation/dedifferentiation and cell plasticity [23]. Stemness of cancer cells lead to enhanced plasticity and play important roles in cancer cell spreading and metastasis [23,24]. Therefore, we further investigated A-P$_{as}$chiRNA's effect on ESCC stemness. The aforementioned cells were subjected to spheroid formation assay, and the results showed that A-P$_{as}$chiRNA depletion or A-P$_{as}$chiRNA overexpression

inhibited or promotes sphere-forming ability, respectively (Fig. 2E). Furthermore, depletion of A-P_{as}chiRNA decreased the proportion of cells labeled with CD44, an ESCC stemness marker [17], while overexpression of A-P_{as}chiRNA significantly increased the proportion of $CD44^+$ cells (Fig. 2F). Consistently, the misexpression of CD44 regulated by A-P_{as}chiRNA was confirmed by immunostaining (Fig. 2G). Together, these results suggested that A-P_{as}chiRNA possessed property of promoting metastatic potency and enhancing cancer stemness in human ESCC.

To understand the mechanism for A-P_{as}chiRNA-regulated ESCC cancer stemness, we conducted an ExProfile qPCR Array that contains 87 known stemness-related genes. 42 genes were downregulated by A-P_{as}chiRNA depletion (more than 2.0 folds) in HKESC-3-shA-P_{as} versus HKESC-3-shCtrl cells and the 15 genes were upregulated by A-P_{as}chiRNA overexpression (more than 2.0 folds) in HKESC-2-A-P_{as} versus HKESC-2-vector cells (Fig. 3A). The overlapping region of Venn diagram represented A-P_{as}chiRNA-regulated genes: OCT4, SOX2, KLF4, KLF5, and CD90 (Fig. 3B). RT-qPCR validated that only OCT4, not the other four, was significantly down- and up-regulated by A-P_{as}chiRNA depletion and overexpression, respectively ($P < 0.001$; Fig. 3C). Immunoblotting further confirmed that A-P_{as}chiRNA regulated OCT4 expression in ESCC cells (Fig. 3D), suggesting that OCT4 was a crucial downstream stemness signature that mediated A-P_{as}chiRNA-promoted ESCC phenotypic characteristics.

3.4. A-P_{as}chiRNA enhances stemness and lymph node metastasis in vivo

To investigate A-P_{as}chiRNA-OCT4 axis on cancer stemness and metastatic potency in vivo, we inoculated HKESC-2-A-P_{as}, HKESC-2-A-P_{as}-shOCT4, and HKESC-2-vector cells into flanks of nude mice. A-P_{as}chiRNA-overexpressing tumors grew faster than the vector tumors did (Fig. 4A). The excised tumors with A-P_{as}chiRNA overexpression were robustly heavier and bigger than the vector tumors when the mice were scarified at the end of the experiment ($P < 0.001$; Fig. 4B, left panel). OCT4 deletion remarkably reversed A-P_{as}chiRNA-induced tumor growth (Fig. 4A and B). Immunostaining with anti-CD44 antibody supported that A-P_{as}chiRNA overexpression enhanced the stemness of primary tumor and the effect of A-P_{as}chiRNA was attenuated by depletion of OCT4 (Fig. 4C).

To further investigate the effect of A-P_{as}chiRNA on lymph node metastasis, aforementioned cells were labeled with luciferase and injected into the flanks of nude mice, which enabled us to monitor the inguinal lymph node metastasis. Mice subcutaneously injected with A-P_{as}chiRNA overexpressing cells developed larger metastatic lesions in inguinal lymph node, than those with vector cells. OCT4 deletion repressed A-P_{as}chiRNA-induced metastatic potency (Fig. 4D). Of note, immunostaining of inguinal lymph nodes isolated from mouse model showed that greater proportion of $CD44^+$ cancer cells were enriched in metastatic lesions from mice subcutaneously injected with A-P_{as}chiRNA overexpression cells, compared with those with vector cells. OCT4 deletion repressed A-P_{as}chiRNA-enhanced $CD44^+$ cancer cells in metastatic lesions (Fig. 4E). These results suggested that A-P_{as}chiRNA was able to enhance ESCC cancer stemness and promoted metastasis through modulating OCT4.

3.5. ERK5-mediated non-canonical PAF1 is required for A-P_{as}chiRNA-promoted cancer stemness

The Polymerase II–associated factor 1 (PAF1) complex (PAF1C), which consists of 5 subunits (PAF1, CDC73, CTR9, LEO1, and SKI8), plays vital roles in gene regulation, and is significantly associated with the development of human diseases [25,26]. PAF1C modulates the release of paused Pol II into productive nucleotide chain elongation [25,27,28]. PAF1 loss leads to aberrant, prematurely terminated transcripts and diminution of full-length transcripts [29]. Recently, increasing evidence has demonstrated that PAF1, in a PAF1C independent manner, has distinct roles in the maintenance of embryonic stem cells (ESCs) and cancer stem cells (CSCs), and in lineage differentiation [30,31]. Elevated expression of PAF1 maintains cancer stemness population and induces tumorigenesis and metastasis in pancreatic and ovarian cancer [30,32,33]. Therefore, a non-canonical function of PAF1, which is complex-independent, is emerging to be linked to cancer stemness.

The role of PAF1 independent on PAF1C in tumorigenesis and maintenance of CSCs-like properties has been emerged [30]. Enhanced PAF1 is accompanied by elevated expression of self-renewal markers (i.e., OCT4, SHH, CD44 and CTNNB1 (β-catenin)) [34]. Knockdown Paf1 led to a decreased expression of Oct4 and other pluripotency markers, accompanied by a loss of mouse embryonic stem cells (ESCs) self-renewal and subsequent differentiation [31]. Gene Expression Omnibus (GEO) dataset (GSE33426) showed higher PAF1 mRNA levels in ESCC compared with their paired normal adjacent tissues ($P < 0.01$; Supplementary Fig. 2A). Furthermore, Pearson correlation analysis

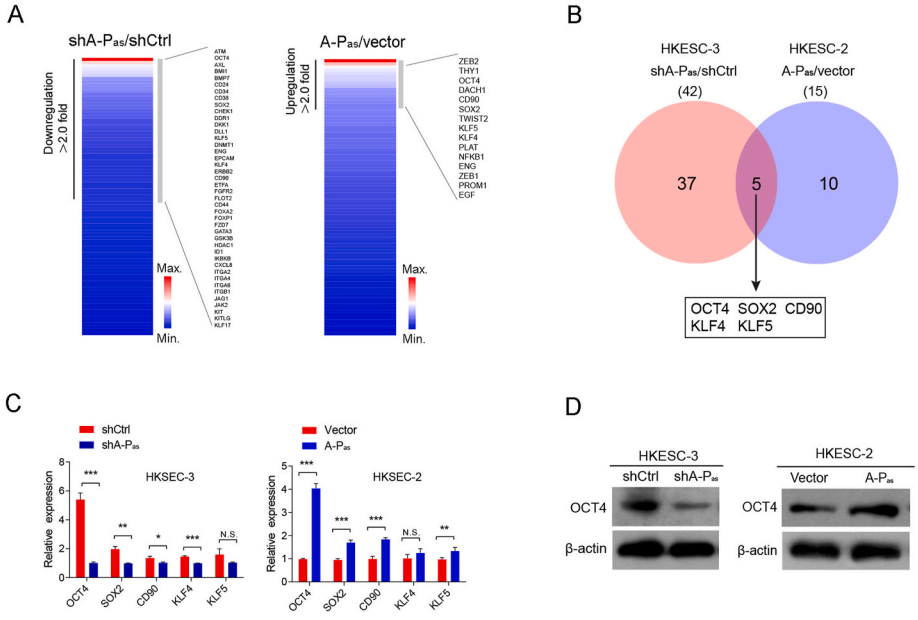

Fig. 3. A-P_{as}chiRNA upregulates OCT4 expression. (a) Heat map showed fold change expression of stemness signatures in HKESC-3-shA-P_{as} cells (left panel) or HKESC-2-A-P_{as} cells (right panel) based on PCR array. (b) Venn diagram showed the overlap of 42 stemness-related genes downregulated by A-P_{as}chiRNA depletion (red), 15 stemness-related genes upregulated by A-P_{as}chiRNA overexpression (blue). Numbers in the overlapping region of Venn diagram represent A-P_{as}chiRNA-regulated genes: OCT4, SOX2, CD90, KLF4 and KLF5. (c) The mRNA levels of five genes (OCT4, SOX2, CD90, KLF4 and KLF5) in HKESC-3-shA-P_{as} cells (left panel) or HKESC-2-A-P_{as} cells (right panel) were determined by RT-qPCR. (d) The protein levels of OCT4 in HKESC-3-shA-P_{as} cells (left panel) or HKESC-2-A-P_{as} cells (right panel) were determined by immunoblotting. β-actin was used as an internal control. Data are shown as the means of three independent experiments or representative data. Error bars indicate SD. N.S., not statistically significant. *$P < 0.05$, **$P < 0.01$, ***$P < 0.001$ by Student's t-test. (For interpretation of the references to color in this figure legend, the reader is referred to the Web version of this article.)

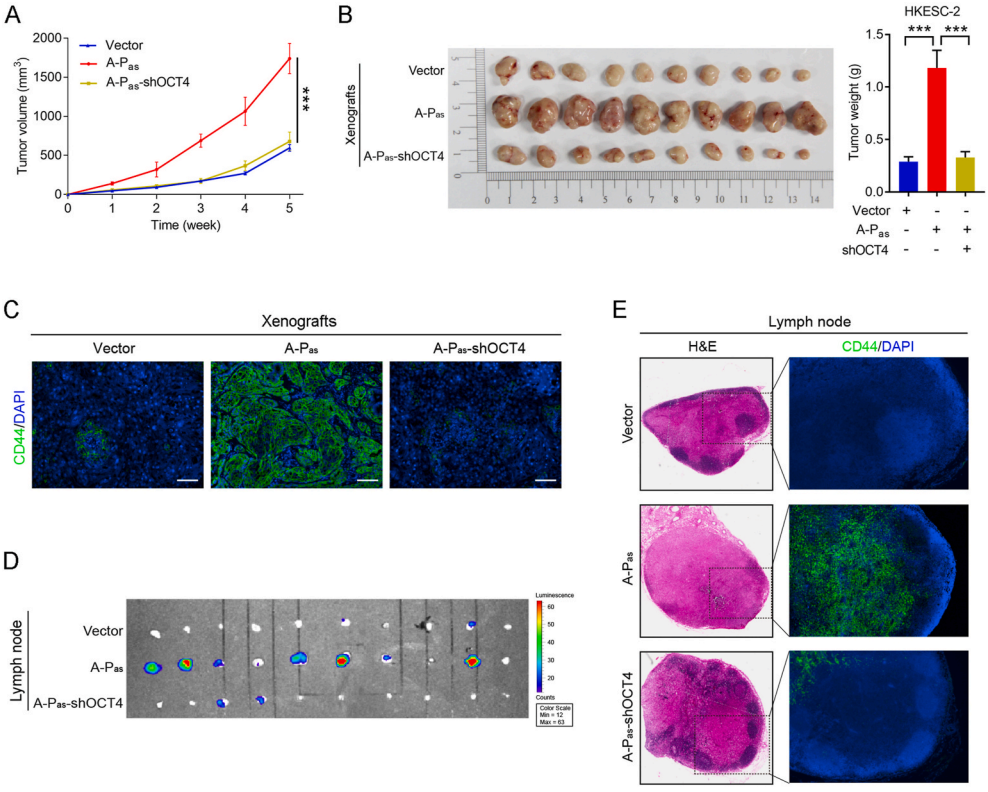

Fig. 4. A-P_{as}chiRNA enhances stemness and lymph node metastasis in vivo. (a) Tumor growth curves showed the measure tumor volumes over time (n = 10). (b) Representative tumors (left panel) and the bar charts of the weights (right panel) of all tumors harvested at the end of the experiments were shown. (c) Immunofluorescent staining of CD44 in tumors derived from mice models were shown. Scale bars: 100 μm. (d) Bioluminescence imaging of the inguinal lymph nodes extracted from mice (n = 10) were shown. (e) H&E (left panel) and immunofluorescence staining of CD44 (right panel) in lymph nodes isolated from mice were shown. Data are shown as the means of three independent experiments or representative data. Error bars indicate SD. ***P < 0.001 by Student's t-test or one-way ANOVA with post hoc intergroup comparisons; in each group.

revealed a significant positive correlation between PAF1 and OCT4 in the GSE33426 dataset (r = 0.4792 and P = 0.0001; Supplementary Fig. 2B). GSEA on dataset GSE29001 and GSE33426 indicated that PAF1 was positively associated with stemness as well as metastasis signatures (P = 0.032, FDR = 0.415; P = 0.008, FDR = 0.512, respectively; Supplementary Fig. 3A and B). We therefore hypothesized that A-P_{as}chiRNA could upregulate PAF1 expression, while PAF1 functions in a PAF1C-independent way subsequently increases the expression of OCT4. Expression of PAF1 was remarkably down- or up-regulated by A-P_{as}chiRNA depletion or overexpression, respectively, as revealed by RT-qPCR and immunoblotting analysis (P < 0.001 for all, Fig. 5A and B). Moreover, cells stably expressing the shRNA of PAF1 largely reversed the OCT4 upregulation induced by A-P_{as}chiRNA (P < 0.01; Fig. 5C). In addition, spheroid formation assay showed that PAF1 depletion successfully reversed the increase in sphere-forming ability induced by A-P_{as}chiRNA overexpression (Fig. 5D). These data suggested that A-P_{as}chiRNA upregulated OCT4 and subsequently promoted cancer stemness depending on non-canonical PAF1 activity.

Next, we exploded the possible mechanism that bridges A-P_{as}chiRNA to PAF1. Sanger sequencing confirmed that A-P_{as}chiRNA is translated into a protein that has the N-terminal portion of the full-length ASTN2 protein and the subsequent 81 new amino acids at the C-terminal portion are in a novel sequence that does not correspond to any part of the PAPPA protein (Fig. 1B). In addition, ribosomes were extracted from

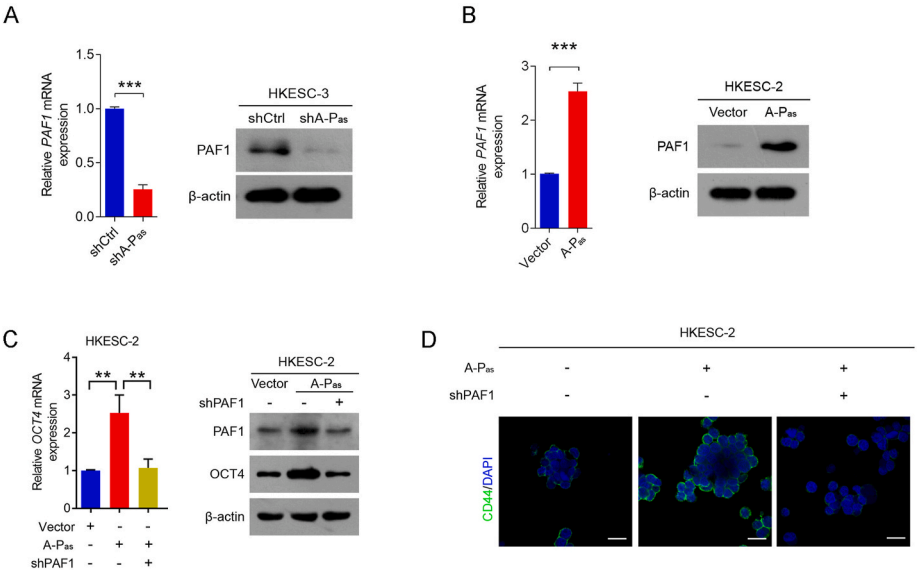

Fig. 5. A-P_{as}chiRNA enhances OCT4 expression via up-regulation PAF1. (a) The mRNA and protein levels of PAF1 in HKESC-3-shA-P_{as} cells were determined by RT-qPCR (left panel) and immunoblotting (right panel). (b) The mRNA and protein level of PAF1 in HKESC-2-A-P_{as} cells were determined by RT-qPCR (left panel) and immunoblotting (right panel). (c) The mRNA and protein level of OCT4 in HKSEC-2 cells stably transfected with A-P_{as}-expressing plasmid or co-transfected with A-P_{as} and shPAF1 were determined by RT-qPCR (left panel) and immunoblotting (right panel). (d) Immunofluorescent staining of CD44 in HKSEC-2 cells stably transfected with A-P_{as}-expressing plasmid or co-transfected with A-P_{as} and shPAF1 was shown. Scale bars: 100 μm. Data are shown as the means of three independent experiments or representative data. Error bars indicate SD. **P < 0.01, ***P < 0.001 by Student's t-test.

HKESC-3 cells and HKESC-2 cells. PCR was further performed and the results showed A-P_{as}chiRNA expression was detected in the ribosomes of HKESC-3 cells, suggesting that A-P_{as}chiRNA can be translated into proteins (Supplementary Fig. 4A). Previous study has reported that the ASTN2 contains three EGF-like domains. Thus, we predicted that A-P_{as}chiRNA translated into a fusion protein contained three EGF-like domains and had a near identical size to the ASTN2 parental protein (Supplementary Fig. 4B). We then speculated that A-P_{as}chiRNA exerted EGF-like actions by modulating its downstream molecules to regulate cancer stemness. Among the known downstream molecules activated by EGF, ERK5 signaling has been reported to be important for promoting cancer stemness and regulating OCT4 [35,36]. Based on the proposed mechanism of the nucleocytoplasmic transport of ERK5 [36,37], phosphorylation of the N-terminal TEY sequence of ERK5 causes the activation of ERK5, resulting in autophosphorylation of its C-terminal region [38]. p-ERK5 in turn enters the nucleus to increase the transcription activity of target molecules [37]. Moreover, analysis of a set of samples from the Oncomine database which includes 53 ESCC specimens revealed that the mRNA levels of ERK5 were significantly elevated in ESCC compared to their paired adjacent normal tissues ($P < 0.001$; Supplementary Fig. 5). Furthermore, GSEA on dataset GSE20347 and GSE43519 indicated that ERK5 was positively associated with stemness and metastasis signatures, respectively ($P < 0.0001$, FDR = 0.645; $P = 0.044$, FDR = 0.929, respectively; Supplementary Fig. 6A and B). Immunoblotting analysis showed that A-P_{as}chiRNA deletion in HKESC-3 cells effectively suppressed the expression of p-ERK5 as well as p-EGFR, PAF1 and OCT4 (Fig. 6A). Conversely, A-P_{as}chiRNA overexpression in HKESC-2 cells was accompanied by increased the expression of p-ERK5 as well as p-EGFR, PAF1 and OCT4 as compared with control (Fig. 6B). To test the hypothesis that EGF-like domain is required for A-P_{as}chiRNA-activated ERK5, EGF-like domains were deleted in HKESC-2-A-P_{as} cells (A-P_{as}-△EGF). A-P_{as}-△EGF abolished A-P_{as}-regulated the expression of PAF1 as well as p-EGFR, p-ERK5 and OCT4 (Fig. 6B). These results were further validated by ERK5 deletion or ERK5 inhibitor in HKESC-2 cells with A-P_{as}chiRNA overexpression. ERK5 knockdown or inhibition drastically rescued A-P_{as}chiRNA-induced PAF1 and OCT4 upregulation (Fig. 6C–F). These data suggested that A-P_{as}chiRNA activated ERK5 that upregulated PAF1, subsequently enhancing OCT4 expression and increasing cancer stemness. Together, these results suggested that ERK5-medicated non-canonical PAF1 activity was required for A-P_{as}chiRNA-promoted cancer stemness (Fig. 6G).

4. Discussion

In this study, we further characterized a chimeric RNA (A-P_{as}chiRNA) that was enriched in human ESCC but not in matched adjacent non-malignant esophagus. The increased level of this chimeric RNA correlated with cancer progression and poor prognosis. Furthermore, A-P_{as}chiRNA promoted the spread of ESCC cells to lymph nodes and enhanced stemness through modulating OCT4 both in vitro and in vivo. Mechanistically, ERK5-mediated non-canonical PAF1 activity was essential for A-P_{as}chiRNA-induced cancer stemness.

To clarify the generation of A-P_{as}chiRNA, we performed the long-range PCR on the genomic DNA, and the absence of size differences between cancer and normal control indicated that there were no large-scale DNA rearrangements. However, a more definitive way to evaluate the possibility of genomic changes (deletion, inversion, and translocation) forming a chimeric gene to produce A-P_{as}chiRNA is deep whole genome sequencing. Until we have the results of genome sequencing, this possibility remains. However, the positive correlation of A-P_{as}chiRNA copy number with ASTN2 gene expression level suggested that A-P_{as}chiRNA formation was under the influence of ASTN2 gene promoter activity. The presence of RNA splice sites on the genomic DNA at the chimeric RNA junction supported the involvement of RNA splicing in the process of forming A-P_{as}chiRNA. Cis-splicing of adjacent genes (cis-SAGe) is a RNA processing event that occurs within a single pre-mRNA, where the transcription machinery reads through the intergenic regions of two neighboring genes and is further spliced at the exons to create the final fusion product [39,40]. Therefore, two likely possible mechanisms remain: 1) transcription read-through of ASTN2 all the way through PAPPA-AS1 to beyond the antisense portion of 18th intron of PAPPA with cis-splicing of the pre-RNA to result in A-P_{as}chiRNA; 2) transcription read-through of PAPPA-AS1 such that the transcript contains the antisense portion of 18th intron of PAPPA with trans-splicing of ASTN2 pre-RNA and the elongated PAPPA-AS1 pre--RNA to produce A-P_{as}chiRNA. To the best of our knowledge, the currently reported A-P_{as}chiRNA could be the first chimeric RNA derived from the splicing of exons and intron antisense of two neighboring genes, respectively.

A-P_{as}chiRNA is expected to be translated into a protein with the N-terminal portion of the full-length ASTN2 protein and a novel sequence of 81 amino acids at the C-terminus. The cDNA sequence fused into A-P_{as}chiRNA that coded for these C-terminal amino acids is derived from the antisense strand of the 18th intron of PAPPA. In this project, we have examined the biological function of this novel protein in the context of cancer stemness in ESCC.

OCT4, SOX2, KLF4, CMYC, and NANOG are the core transcription factors that regulate pluripotency and stemness, and their ectopic expression in human and murine fibroblasts induces pluripotent stem cell formation [41,42]. Among these transcription factors, OCT4 is well established as a master factor controlling the self-renewal and pluripotency of cancer stem cells [43]. Previous studies have reported that elevated OCT4 expression not only promotes EMT, invasion, and migration of ESCC cells, but also acts as a predictor of poor prognosis in ESCC patients [44]. In this study, we revealed that A-P_{as}chiRNA unregulated OCT4 expression to enhance ESCC cancer stemness, and promote metastatic potency in vitro and ESCC cells spreading to lymph in vivo. This is the first report that the abnormal expression of chimeric RNA is described to induce the characteristics of the cancer stem cells. Further investigation is required to clarify the role of fusion protein encoded by A-P_{as}chiRNA to the molecular mechanisms underlying the connection between A-P_{as} fusion protein and the cancer stemness.

Emerging evidence suggests that ERK5-mediated signaling promotes the cancer stemness and metastasis in a wide variety of cancers including breast, colon, lung and prostate cancers [36,45–47]. ERK5 is activated by several extracellular stimuli, such as stress and growth factors, and has an important role in several cellular responses [36]. Previously study reported that treatment with hormone elicits recruitment of p-ERK5 and PAF1 to the TSS of 17β-estradiol-regulated genes and regulation of gene expression, especially of genes that control cell proliferation in breast cancer [48]. Our study found that the translation product of the A-P_{as}chiRNA possessed EGF-like domains, which upregulated PAF1 via ERK5 to promote cancer stemness characteristics. ERK5 activation serves as a bridge to link A-P_{as}chiRNA and PAF1. PAF1 is involved in many important cellular events, particularly those related to self-renewal and pluripotency, and its deregulation is associated with cancer stemness [30]. Previous studies reported that the importance of non-canonical PAF1 in maintenance of self-renewal of CSCs implicate PAF1 as an attractive target for combating CSC-mediated tumor progression and recurrence [33]. Thus far, no relationship has been established between ESCC cancer stem-like phenotypes and non-canonical PAF1 activity. Here, we demonstrated that ERK5-medicated non-canonical PAF1 activity could contribute to the maintenance of a stem-like population in ESCC. A-P_{as}chiRNA activates ERK5 that upregulates PAF1, subsequently enhancing OCT4 expression and increasing cancer stemness. Future studies are necessary to evaluate the impact of A-P_{as}chiRNA-promoted ESCC stemness using multi-level verification (i.e., patient-derived in vitro and in vivo models, genetically engineered mouse models).

In summary, this study defined for the first time that the A-P_{as}chiRNA aggravates cancer progression and cancer cell spreading. The

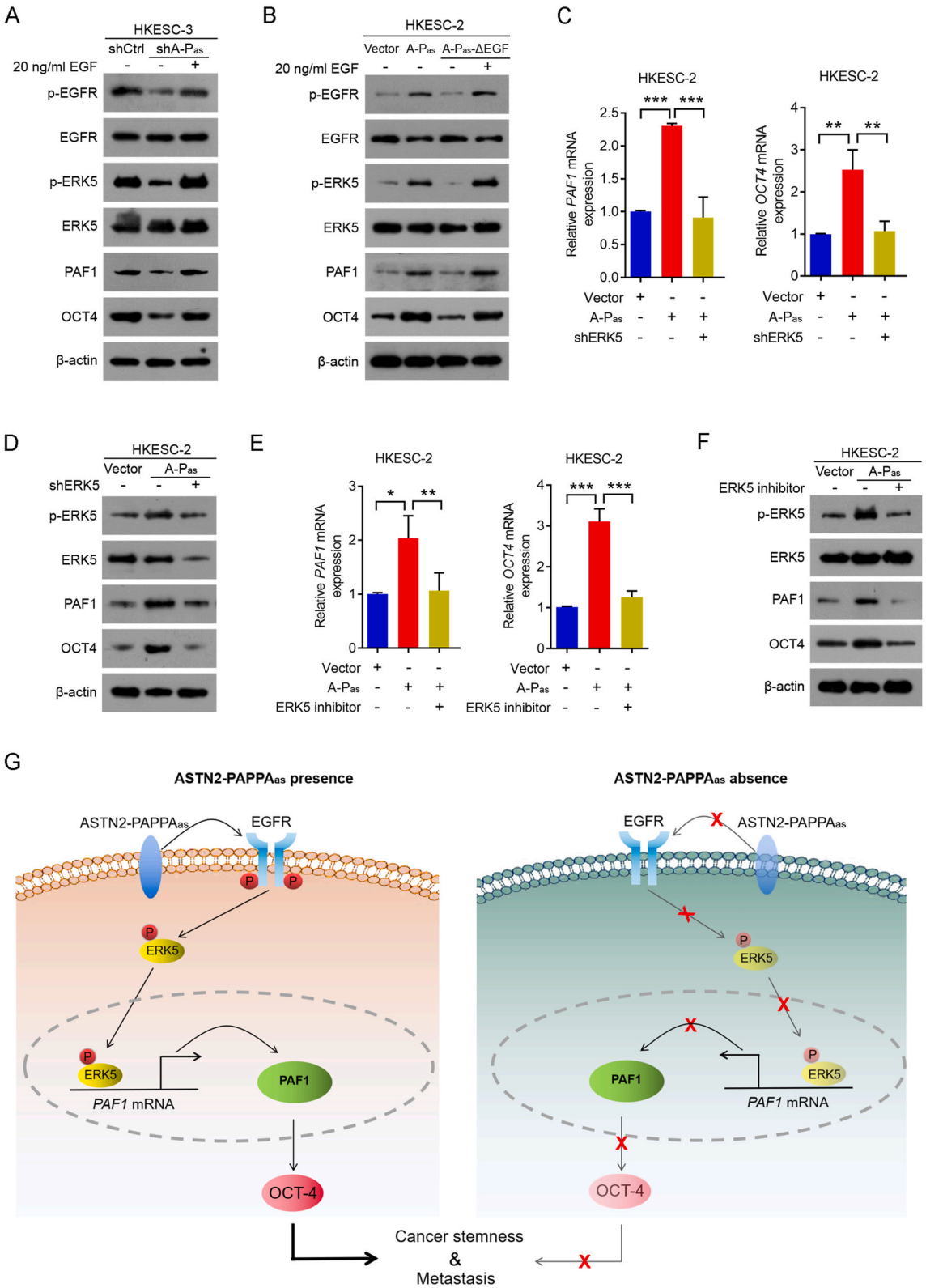

Fig. 6. ERK5-medicated non-canonical PAF1 activity is required for A-P_{as}chiRNA-promoted cancer stemness. (a) Immunoblotting of p-EGFR, EGFR, p-ERK5, ERK5, PAF1, OCT4 in HKESC-3-shA-P_{as} cells incubated with or without EGF was shown. (b) Immunoblotting of p-EGFR, EGFR, p-ERK5, ERK5, PAF1, OCT4 in HKESC-2-vector, HKESC-2-A-P_{as}, HKESC-2-A-P_{as}-△EGF incubated with or without EGF was shown. (c) RT-qPCR of PAF1 (left panel) and OCT4 (right panel) in HKESC-2-vector, HKESC-2-A-P_{as}, HKESC-2 cells co-transfected with A-P_{as} and shERK5 was shown. (d) Immunoblotting of p-ERK5, ERK5, PAF1, OCT4 in HKSEC-2 cells stably transfected with A-P_{as} plasmid or co-transfected with A-P_{as} and shERK5 was shown. (e) RT-qPCR of PAF1 (left panel) and OCT4 (right panel) in HKESC-2-A-P_{as} cells incubated with or without ERK5 inhibitor. (f) Immunoblotting of p-ERK5, ERK5, PAF1, OCT4 in HKESC-2-A-P_{as} cells incubated with or without ERK5 inhibitor was shown. (g) Schematic summary of the role of ASTN2-PAPPA$_{as}$ in esophageal squamous cell carcinoma. Data are shown as the means of three independent experiments or representative data. Error bars indicate SD. *P < 0.05, **P < 0.01, ***P < 0.001 by Student's t-test.

currently reported A-P_{as}chiRNA could be the first chimeric RNA derived from the splicing of exons and intron antisense of two neighboring genes, respectively. Our data also illustrate that A-P_{as}chiRNA acts as a prognostic marker for poor survival in ESCC.

Authors' contributions

H.Z. conceived and designed the experiments. X.X. and Z.Y. performed bioinformatics analyses. L.W., J.Z, K.L. and J.G. performed the in vitro experiments. L.W. and X.X. performed the in vivo experiments. L. W. and Y.L. performed and guided the statistical analysis. Y.G., Y.C., F. Z., Y.P., J.F. and Y.C. provided or collected the study materials or patients; H.Z., S.-C.J.Y. and S.G. wrote the manuscript. All the authors read and approved the final manuscript.

Declaration of competing interest

The authors declare that they have no competing interests.

Acknowledgements

Authors want to thank Dr. L.S. Yen for the discussion and technical help. We acknowledge members of H. Zhang's laboratory for the technical help and discussion. The work was supported in part by the National Natural Science Foundation of China (82072683, 81773087, 81071736, 81572876 and 30973508 to H.Z.; 82002491 to L.W.); the Natural Science Foundation of Guangdong Province of China (9151018004000000 to H.Z.); the Science and Technology Planning Project of Guangdong Province of China (2019A030317024 to H.Z.); Special Project on the Integration of Industry, Education and Research of Guangdong Province (2011A090100024 to H.Z.); China Postdoctoral Science Foundation (2020M673078 to L.W.); Flagship specialty construction project-General surgery (Funding No.:711003).

Appendix A. Supplementary data

Supplementary data to this article can be found online at https://doi.org/10.1016/j.canlet.2020.10.052.

References

[1] H. Wu, X. Li, H. Li, Gene fusions and chimeric RNAs, and their implications in cancer, Genes Dis. 6 (2019) 385–390.
[2] T.H. Rabbitts, Chromosomal translocations in human cancer, Nature 372 (1994) 143–149.
[3] M. Babiceanu, F. Qin, Z. Xie, Y. Jia, K. Lopez, N. Janus, L. Facemire, S. Kumar, Y. Pang, Y. Qi, I.M. Lazar, H. Li, Recurrent chimeric fusion RNAs in non-cancer tissues and cells, Nucleic Acids Res. 44 (2016) 2859–2872.
[4] S.K. Gupta, L. Luo, L. Yen, RNA-mediated gene fusion in mammalian cells, Proc. Natl. Acad. Sci. U. S. A. 115 (2018) E12295–E12304.
[5] Y. Lin, H. Dong, W. Deng, W. Lin, K. Li, X. Xiong, Y. Guo, F. Zhou, C. Ma, Y. Chen, H. Ren, H. Yang, N. Dai, L. Ma, S.J. Meltzer, S.J. Yeung, H. Zhang, Evaluation of salivary exosomal chimeric GOLM1-NAA35 RNA as a potential biomarker in esophageal carcinoma, Clin. Canc. Res. 25 (2019) 3035–3045.
[6] Z. Xie, M. Babiceanu, S. Kumar, Y. Jia, F. Qin, F.G. Barr, H. Li, Fusion transcriptome profiling provides insights into alveolar rhabdomyosarcoma, Proc. Natl. Acad. Sci. U. S. A. 113 (2016) 13126–13131.
[7] H. Zhang, W. Lin, K. Kannan, L. Luo, J. Li, P.W. Chao, Y. Wang, Y.P. Chen, J. Gu, L. Yen, Aberrant chimeric RNA GOLM1-MAK10 encoding a secreted fusion protein as a molecular signature for human esophageal squamous cell carcinoma, Oncotarget 4 (2013) 2135–2143.
[8] J. Lagergren, E. Smyth, D. Cunningham, P. Lagergren, Oesophageal cancer, Lancet 390 (2017) 2383–2396.
[9] K. Kannan, L. Wang, J. Wang, M.M. Ittmann, W. Li, L. Yen, Recurrent chimeric RNAs enriched in human prostate cancer identified by deep sequencing, Proc. Natl. Acad. Sci. U. S. A. 108 (2011) 9172–9177.
[10] P.M. Wilson, R.H. Fryer, Y. Fang, M.E. Hatten, Astn2, a novel member of the astrotactin gene family, regulates the trafficking of ASTN1 during glial-guided neuronal migration, J. Neurosci. 30 (2010) 8529–8540.
[11] J.T. Glessner, K. Wang, G. Cai, O. Korvatska, C.E. Kim, S. Wood, H. Zhang, A. Estes, C.W. Brune, J.P. Bradfield, M. Imielinski, E.C. Frackelton, J. Reichert, E. L. Crawford, J. Munson, P.M. Sleiman, R. Chiavacci, K. Annaiah, K. Thomas, C. Hou, W. Glaberson, J. Flory, F. Otieno, M. Garris, L. Soorya, L. Klei, J. Piven, K. J. Meyer, E. Anagnostou, T. Sakurai, R.M. Game, D.S. Rudd, D. Zurawiecki, C. J. McDougle, L.K. Davis, J. Miller, D.J. Posey, S. Michaels, A. Kolevzon, J. M. Silverman, R. Bernier, S.E. Levy, R.T. Schultz, G. Dawson, T. Owley, W. M. McMahon, T.H. Wassink, J.A. Sweeney, J.I. Nurnberger, H. Coon, J.S. Sutcliffe, N.J. Minshew, S.F. Grant, M. Bucan, E.H. Cook, J.D. Buxbaum, B. Devlin, G. D. Schellenberg, H. Hakonarson, Autism genome-wide copy number variation reveals ubiquitin and neuronal genes, Nature 459 (2009) 569–573.
[12] A.C. Lionel, J. Crosbie, N. Barbosa, T. Goodale, B. Thiruvahindrapuram, J. Rickaby, M. Gazzellone, A.R. Carson, J.L. Howe, Z. Wang, J. Wei, A.F. Stewart, R. Roberts, R. McPherson, A. Fiebig, A. Franke, S. Schreiber, L. Zwaigenbaum, B.A. Fernandez, W. Roberts, P.D. Arnold, P. Szatmari, C.R. Marshall, R. Schachar, S.W. Scherer, Rare copy number variation discovery and cross-disorder comparisons identify risk genes for ADHD, Sci. Transl. Med. 3 (2011), 95ra75.
[13] J.B. Lawrence, C. Oxvig, M.T. Overgaard, L. Sottrup-Jensen, G.J. Gleich, L.G. Hays, J.R. Yates 3rd, C.A. Conover, The insulin-like growth factor (IGF)-dependent IGF binding protein-4 protease secreted by human fibroblasts is pregnancy-associated plasma protein-A, Proc. Natl. Acad. Sci. U. S. A. 96 (1999) 3149–3153.
[14] C.A. Conover, C. Oxvig, -A. Papp, A promising therapeutic target for healthy longevity, Aging Cell 16 (2017) 205–209.
[15] D. Donegan, L.K. Bale, C.A. Conover, PAPP-A in normal human mesangial cells: effect of inflammation and factors related to diabetic nephropathy, J. Endocrinol. 231 (2016) 71–80.
[16] C.A. Conover, C. Oxvig, PAPP-A and cancer, J. Mol. Endocrinol. 61 (2018) T1–T10.
[17] L. Du, L. Wang, J. Gan, Z. Yao, W. Lin, J. Li, Y. Guo, Y. Chen, F. Zhou, S.C. Jim Yeung, R.P. Coppes, D. Zhang, H. Zhang, MTA3 represses cancer stemness by targeting the SOX2OT/SOX2 Axis, iScience 22 (2019) 353–368.
[18] X. Xiong, X. Ke, L. Wang, Z. Yao, Y. Guo, X. Zhang, Y. Chen, C.P. Pang, A. V. Schally, H. Zhang, Splice variant of growth hormone-releasing hormone receptor drives esophageal squamous cell carcinoma conferring a therapeutic target, Proc. Natl. Acad. Sci. U. S. A. 117 (2020) 6726–6732.
[19] L. Wang, K. Li, X. Lin, Z. Yao, S. Wang, X. Xiong, Z. Ning, J. Wang, X. Xu, Y. Jiang, D. Liu, Y. Chen, D. Zhang, H. Zhang, Metformin induces human esophageal carcinoma cell pyroptosis by targeting the miR-497/PELP1 axis, Canc. Lett. 450 (2019) 22–31.
[20] H. Dong, J. Xu, W. Li, J. Gan, W. Lin, J. Ke, J. Jiang, L. Du, Y. Chen, X. Zhong, D. Zhang, S.J. Yeung, X. Li, H. Zhang, Reciprocal androgen receptor/interleukin-6 crosstalk drives oesophageal carcinoma progression and contributes to patient prognosis, J. Pathol. 241 (2017) 448–462.
[21] Y. Feng, C. Ke, Q. Tang, H. Dong, X. Zheng, W. Lin, J. Ke, J. Huang, S.C. Yeung, H. Zhang, Metformin promotes autophagy and apoptosis in esophageal squamous cell carcinoma by downregulating Stat3 signaling, Cell Death Dis. 5 (2014), e1088.
[22] S. Wang, Y. Lin, X. Xiong, L. Wang, Y. Guo, Y. Chen, S. Chen, G. Wang, P. Lin, H. Chen, S.J. Yeung, E. Bremer, H. Zhang, Low-dose Metformin Reprograms the Tumor Immune Microenvironment in Human Esophageal Cancer: Results of a Phase II Clinical Trial, 2020. Clin Cancer Res.
[23] N.K. Lytle, A.G. Barber, T. Reya, Stem cell fate in cancer growth, progression and therapy resistance, Nat. Rev. Canc. 18 (2018) 669–680.
[24] J.E. Visvader, G.J. Lindeman, Cancer stem cells: current status and evolving complexities, Cell Stem Cell 10 (2012) 717–728.
[25] N.J. Krogan, M. Kim, S.H. Ahn, G. Zhong, M.S. Kobor, G. Cagney, A. Emili, A. Shilatifard, S. Buratowski, J.F. Greenblatt, RNA polymerase II elongation factors of Saccharomyces cerevisiae: a targeted proteomics approach, Mol. Cell Biol. 22 (2002) 6979–6992.
[26] Y. Xie, M. Zheng, X. Chu, Y. Chen, H. Xu, J. Wang, H. Zhou, J. Long, Paf1 and Ctr9 subcomplex formation is essential for Paf1 complex assembly and functional regulation, Nat. Commun. 9 (2018) 3795.
[27] J. Kim, M. Guermah, R.G. Roeder, The human PAF1 complex acts in chromatin transcription elongation both independently and cooperatively with SII/TFIIS, Cell 140 (2010) 491–503.
[28] F.X. Chen, P. Xie, C.K. Collings, K. Cao, Y. Aoi, S.A. Marshall, E.J. Rendleman, M. Ugarenko, P.A. Ozark, A. Zhang, R. Shiekhattar, E.R. Smith, M.Q. Zhang, A. Shilatifard, PAF1 regulation of promoter-proximal pause release via enhancer activation, Science 357 (2017) 1294–1298.
[29] L. Hou, Y. Wang, Y. Liu, N. Zhang, I. Shamovsky, E. Nudler, B. Tian, B.D. Dynlacht, Paf1C regulates RNA polymerase II progression by modulating elongation rate, Proc. Natl. Acad. Sci. U. S. A. 116 (2019) 14583–14592.
[30] S. Karmakar, P. Dey, A.P. Vaz, S.R. Bhaumik, M.P. Ponnusamy, S.K. Batra, PD2/PAF1 at the crossroads of the cancer network, Canc. Res. 78 (2018) 313–319.
[31] L. Ding, M. Paszkowski-Rogacz, A. Nitzsche, M.M. Slabicki, A.K. Heninger, I. de Vries, R. Kittler, M. Junqueira, A. Shevchenko, H. Schulz, N. Hubner, M.X. Doss, A. Sachinidis, J. Hescheler, R. Iacone, K. Anastassiadis, A.F. Stewart, M. T. Pisabarro, A. Caldarelli, I. Poser, M. Theis, F. Buchholz, A genome-scale RNAi screen for Oct4 modulators defines a role of the Paf1 complex for embryonic stem cell identity, Cell Stem Cell 4 (2009) 403–415.
[32] N. Moniaux, C. Nemos, B.M. Schmied, S.C. Chauhan, S. Deb, K. Morikane, A. Choudhury, M. Vanlith, M. Sutherlin, J.M. Sikela, M.A. Hollingsworth, S. K. Batra, The human homologue of the RNA polymerase II-associated factor 1 (hPaf1), localized on the 19q13 amplicon, is associated with tumorigenesis, Oncogene 25 (2006) 3247–3257.
[33] R.K. Nimmakayala, P. Seshacharyulu, I. Lakshmanan, S. Rachagani, S. Chugh, S. Karmakar, S. Rauth, R. Vengoji, P. Atri, G.A. Talmon, S.M. Lele, L.M. Smith, I. Thapa, D. Bastola, M.M. Ouellette, S.K. Batra, M.P. Ponnusamy, Cigarette smoke induces stem cell features of pancreatic cancer cells via PAF1, Gastroenterology 155 (2018) 892–908, e896.

[34] A.P. Vaz, M.P. Ponnusamy, S. Rachagani, P. Dey, A.K. Ganti, S.K. Batra, Novel role of pancreatic differentiation 2 in facilitating self-renewal and drug resistance of pancreatic cancer stem cells, Br. J. Canc. 111 (2014) 486–496.
[35] D.M. Pereira, S.E. Gomes, P.M. Borralho, C.M.P. Rodrigues, MEK5/ERK5 activation regulates colon cancer stem-like cell properties, Cell Death Dis. 5 (2019) 68.
[36] B. Stecca, E. Rovida, Impact of ERK5 on the hallmarks of cancer, Int. J. Mol. Sci. 20 (2019).
[37] S. Nishimoto, E. Nishida, MAPK signalling: ERK5 versus ERK1/2, EMBO Rep. 7 (2006) 782–786.
[38] H. Morimoto, K. Kondoh, S. Nishimoto, K. Terasawa, E. Nishida, Activation of a C-terminal transcriptional activation domain of ERK5 by autophosphorylation, J. Biol. Chem. 282 (2007) 35449–35456.
[39] K. Jividen, H. Li, Chimeric RNAs generated by intergenic splicing in normal and cancer cells, Genes Chromosomes Cancer 53 (2014) 963–971.
[40] Y. Jia, Z. Xie, H. Li, Intergenically spliced chimeric RNAs in cancer, Trends Canc. 2 (2016) 475–484.
[41] X. Chen, H. Xu, P. Yuan, F. Fang, M. Huss, V.B. Vega, E. Wong, Y.L. Orlov, W. Zhang, J. Jiang, Y.H. Loh, H.C. Yeo, Z.X. Yeo, V. Narang, K.R. Govindarajan, B. Leong, A. Shahab, Y. Ruan, G. Bourque, W.K. Sung, N.D. Clarke, C.L. Wei, H. H. Ng, Integration of external signaling pathways with the core transcriptional network in embryonic stem cells, Cell 133 (2008) 1106–1117.
[42] M. Abad, L. Mosteiro, C. Pantoja, M. Canamero, T. Rayon, I. Ors, O. Grana, D. Megias, O. Dominguez, D. Martinez, M. Manzanares, S. Ortega, M. Serrano, Reprogramming in vivo produces teratomas and iPS cells with totipotency features, Nature 502 (2013) 340–345.
[43] A. Radzisheuskaya, B. Chia Gle, R.L. dos Santos, T.W. Theunissen, L.F. Castro, J. Nichols, J.C. Silva, A defined Oct4 level governs cell state transitions of pluripotency entry and differentiation into all embryonic lineages, Nat. Cell Biol. 15 (2013) 579–590.
[44] X. Zhou, G.R. Huang, P. Hu, Over-expression of Oct4 in human esophageal squamous cell carcinoma, Mol. Cell. 32 (2011) 39–45.
[45] L. Fulford, D. Milewski, V. Ustiyan, N. Ravishankar, Y. Cai, T. Le, S. Masineni, S. Kasper, B. Aronow, V.V. Kalinichenko, T.V. Kalin, The transcription factor FOXF1 promotes prostate cancer by stimulating the mitogen-activated protein kinase ERK5, Sci. Signal. 9 (2016) ra48.
[46] W. Jiang, F. Cai, H. Xu, Y. Lu, J. Chen, J. Liu, N. Cao, X. Zhang, X. Chen, Q. Huang, H. Zhuang, Z.C. Hua, Extracellular Signal Regulated Kinase 5 Promotes Cell Migration, Invasion and Lung Metastasis in a FAK-dependent Manner, Protein Cell, 2020.
[47] A.E. Simoes, D.M. Pereira, S.E. Gomes, H. Brito, T. Carvalho, A. French, R. E. Castro, C.J. Steer, S.N. Thibodeau, C.M. Rodrigues, P.M. Borralho, Aberrant MEK5/ERK5 signalling contributes to human colon cancer progression via NF-kappaB activation, Cell Death Dis. 6 (2015), e1718.
[48] Z. Madak-Erdogan, R. Ventrella, L. Petry, B.S. Katzenellenbogen, Novel roles for ERK5 and cofilin as critical mediators linking ERalpha-driven transcription, actin reorganization, and invasiveness in breast cancer, Mol. Canc. Res. 12 (2014) 714–727.